A New Nitrogen Pd(II) Complex Immobilized on Magnetic Mesoporous Silica: A Retrievable Catalyst for C–C Bond Formation

Samira Mousavi[1] · Yagoub Mansoori[1] · Ayat Nuri[1] · Behzad Koohi-Zargar[2]

Abstract

A new nitrogen ligand, i.e. 1,3-di-(*o*-aminophenoxy)-2-propyl propargyl ether (DPPE), has been synthesized and characterized. Magnetic mesoporous silica composite (MNP@SiO$_2$-SBA) was obtained via embedding magnetite nano-particles (MNPs) between SBA-15 channels. DPPE palladium dichloride (MNP@SiO$_2$-SBA-DPPE-Pd(II)) was then prepared via click chemistry and fully characterized. The activity and recyclability of supported magnetic Pd(II) catalyst were evaluated in Heck coupling reaction after optimizing the optimal reaction conditions including solvent, amount of catalyst, base and temperature. Aryl iodides and aryl bromides showed enhanced activity compared to those of aryl chlorides in the Heck reaction. The catalyst was easily separated magnetically, reused in five runs sequentially, and no significant loss of activity was observed.

Graphic Abstract
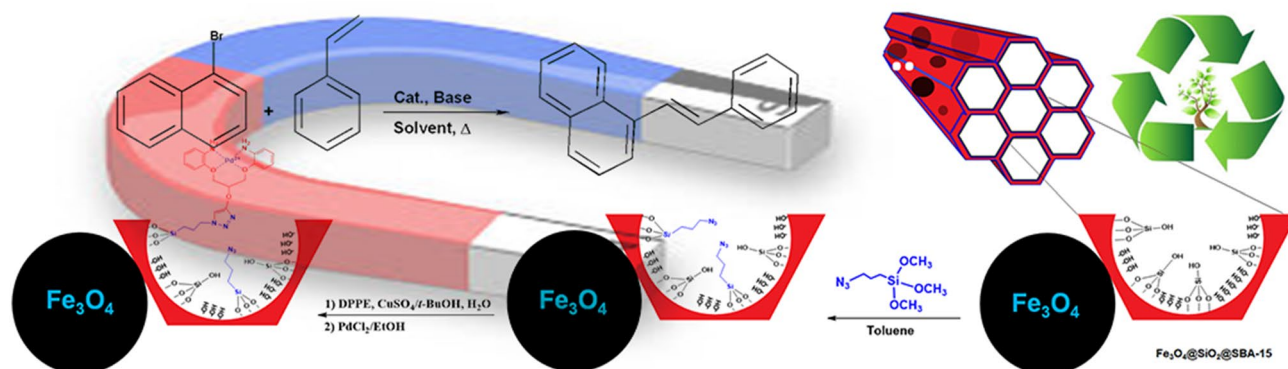
Keywords Click reaction · Magnetic mesoporous silica · Heck reaction · Heterogenized catalyst

✉ Yagoub Mansoori
ya_mansoori@yahoo.com; ya_mansoori@uma.ac.ir

[1] Department of Applied Chemistry, Faculty of Science, University of Mohaghegh Ardabili, Ardabil, Iran

[2] Farabi Chemical and Medical Laboratory, Sarcheshmeh Sq., Shams Alley, Farabi Building, Ardabil, Iran

1 Introduction

Heck, Hiyama, Suzuki, Sonogashira, and Stille cross-coupling reactions are those reactions that they are widely used for C–C bond formation in the modern organic synthesis [1]. The palladium-catalyzed arylation reaction of olefinic compounds with aryl iodides in the presence of potassium acetate was independently reported by Mizoroki [2] and Heck [3] and then developed by Heck, Scheme 1.
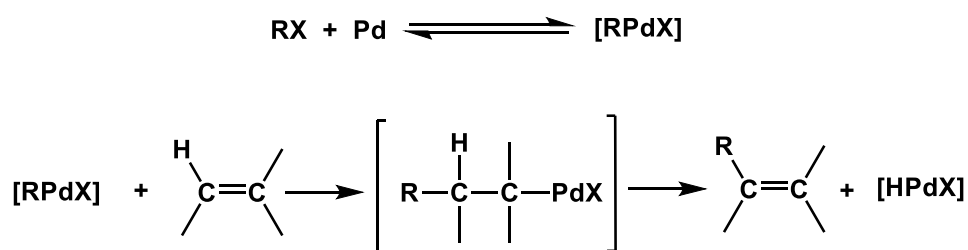
Aryl, benzyl, and styryl halides were found to undergo the reaction however, among the aryl compounds only

Scheme 1 Mizoroki–Heck reaction

$$RX + Pd \rightleftharpoons [RPdX]$$


the iodides reacted rapidly [3]. Among various metals for catalyzing these reactions, palladium is more preferred and widely used due to enhanced activity and selectivity [4]. The Heck reaction is one of the most noted transformations within the Pd-involved organic preparations. Nowadays, Heck-type chemistry is a known method to assemble molecules via the formation of C–C bonds in both conventional and modern organic syntheses [5]. The reaction has a great potential for industrial applications, however, due to the properties and activities of the existing catalysts, limited

industrial applications have been observed for the Heck reaction [6]. During the last decades, the preparation of a broad spectrum of supported Pd(II) complexes with different ligands as catalysts for coupling reactions have been reported. Improving the reaction yields and decreasing reactions time, processes costs, and byproducts are some of the results of these investigations [7].

In recent years, anchoring catalysts on MNPs has been extensively studied [8–11]. Magnetite nanoparticles are nontoxic, highly dispersible, biocompatible, and they have a
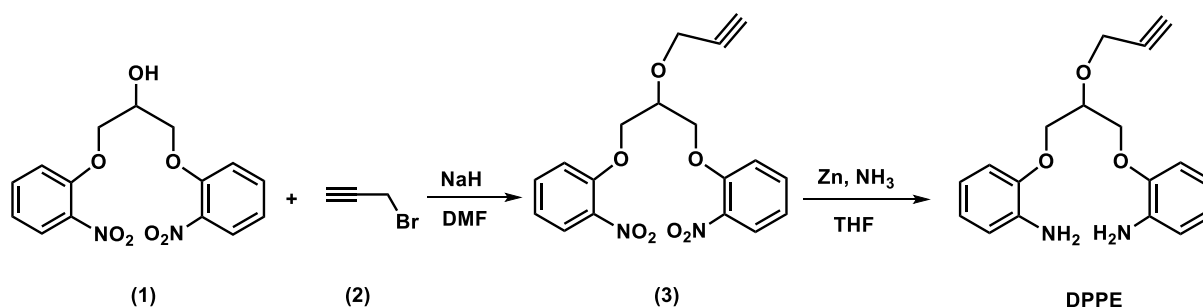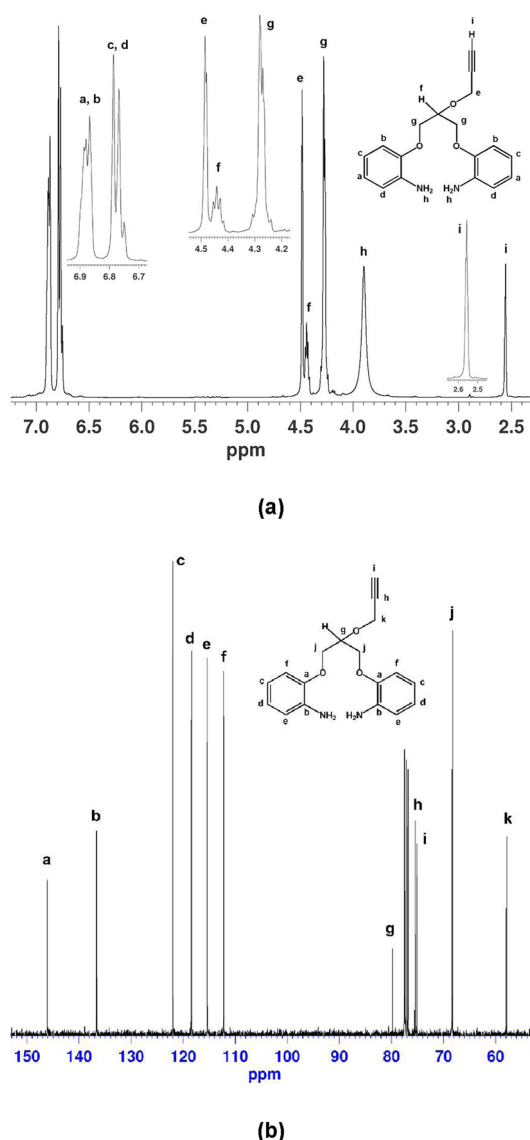

Scheme 2 Synthesis of DPPE

Fig. 1 Mass spectra of DPPE
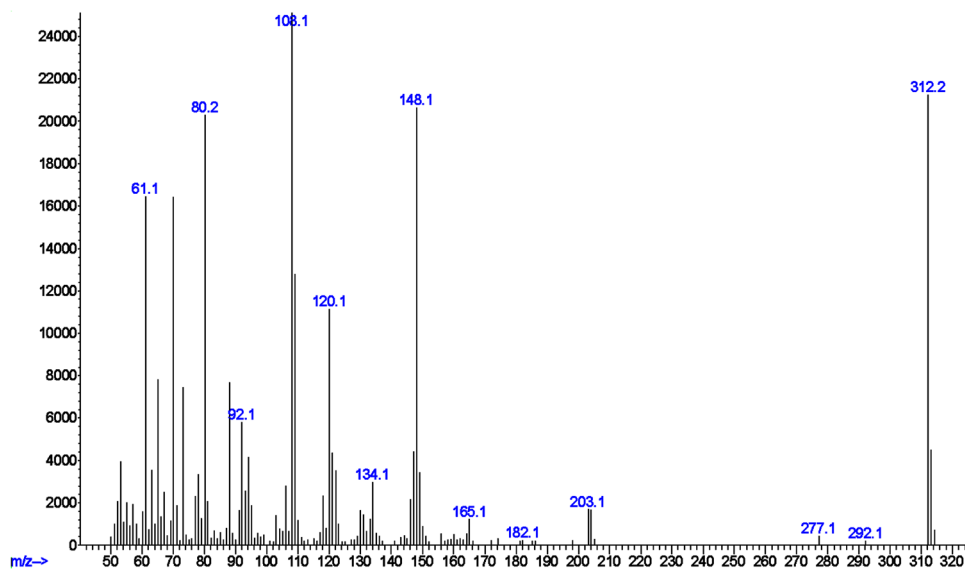
Fig. 2 a ^{1}H NMR (250 MHz) and **b** ^{13}C NMR spectra (62.5 MHz) of DPPE in CDCl$_3$

high surface-to-volume ratio. Furthermore, MNP-supported catalysts enjoy the benefit of easy and rapid magnetic separation from different reaction mixtures [12–14].

It is highly recommended to coat MNPs prior to any treatment because they agglomerate intrinsically due to strong magnetic dipole–dipole interactions and high specific surface area [15, 16]. The most popular method to overcome this problem is using MNPs in the form of a composite with other metal oxides. Compositions of MNPs with different forms of mesoporous silica such as MCMs and SBAs have been widely investigated in recent years [17, 18]. This combination will also give the advantages of both mesoporous materials and magnetic nanoparticles to the MNP/silica

nanocomposite materials. High selectivity and activity by providing high density of single reaction sites via heterogenization of homogenous catalysts, and easy catalyst separation and reusability are some of these advantages [19, 20].

There are plenty of reports on the incorporation of magnetic mesoporous particles as support for catalyst and preparing magnetically retrievable catalyst supports in the literature [14, 21]. For example, Fu et al. reported that magnetic mesoporous silica functionalized with poly(*m*-aminothiophenol) can rapidly adsorb Hg(II) ions. They showed that, the Hg(II)-complexed adsorbent can be used as an efficient catalyst for transformation of phenylacetylene to acetophenone [22]. In another work, Jiang et al. supported the polyoxometalate-based ionic liquid [(C$_4$H$_9$)$_3$NCH$_3$]$_3$PM o$_{12}$O$_{40}$ with short carbon chain onto magnetic mesoporous silica microspheres with rough surface. The prepared catalyst showed enhanced activity toward oxidative desulfurization of diesel with H$_2$O$_2$ as an oxidant in compared with the smooth surface catalyst [23]. Sorokina et al. reported that, pyridylphenylene dendrons immobilized on to magnetic mesoporous silica act as efficient stabilizing molecules of Pd species. Their amphiphilic nanocomposite demonstrates excellent performance in Suzuki–Miyaura cross-coupling reaction in the ethanol/water mixture due to the combination of hydrophilic support and hydrophobic dendrons [24].

Among the Pd-involved organic preparations, the Heck reaction is one of the most noted transformations. Nowadays, Heck-type chemistry is a well-known method to assemble molecules via the formation of C–C bonds in both common and modern organic syntheses [5, 25]. In recent years, the preparation of a wide spectrum of supported Pd(II) complexes with different ligands as catalysts for coupling reactions has been reported. Improving the reaction yields and decreasing reactions time, processes costs, and byproducts are some of the results of these investigations [26, 27].

In the present study, a new ligand, i.e. 1,3-di-(*o*-aminophenoxy)-2-propyl propargyl ether (DPPE), has been synthesized and characterized. The prepared ligand can be supported on the surface of metal oxides via a simple click reaction. Separately, magnetic mesoporous silica was obtained via embedding the MNPs between mesoporous silica channels and then functionalized with azide. The combination of SBA-15 porous structure with the magnetic property of MNPs provides high density of catalytic sites for enhanced activity along with the advantage of simple magnetic decantation of the catalyst at the end of reaction. DPPE was grafted onto the surface via click reaction and then treated with a Pd(II) solution in EtOH to give a new Pd(II)-supported magnetic catalyst (MNP@SiO$_2$-SBA-DPPE-Pd(II)). The obtained magnetic catalyst is a quite effective catalyst in the Heck reaction. Furthermore, it is compatible with the green chemistry principles and can be
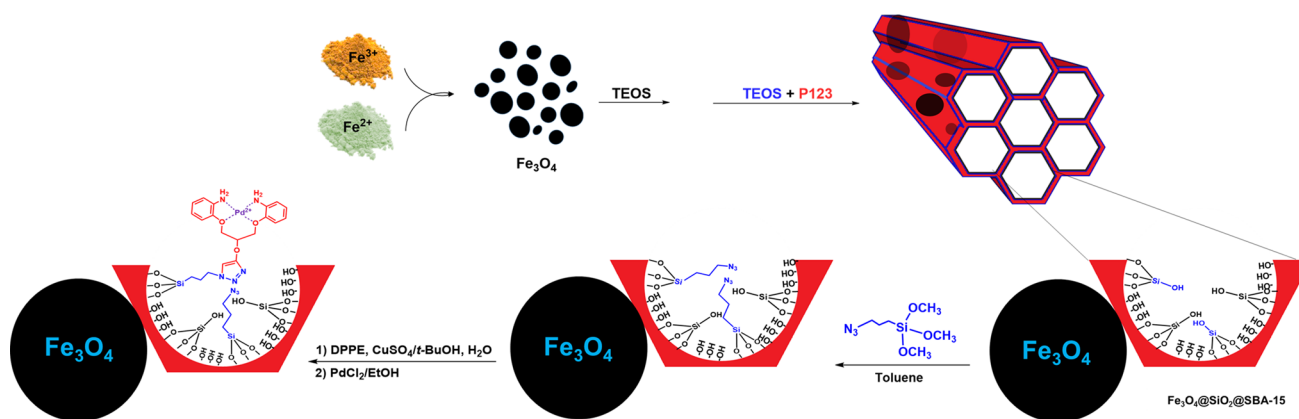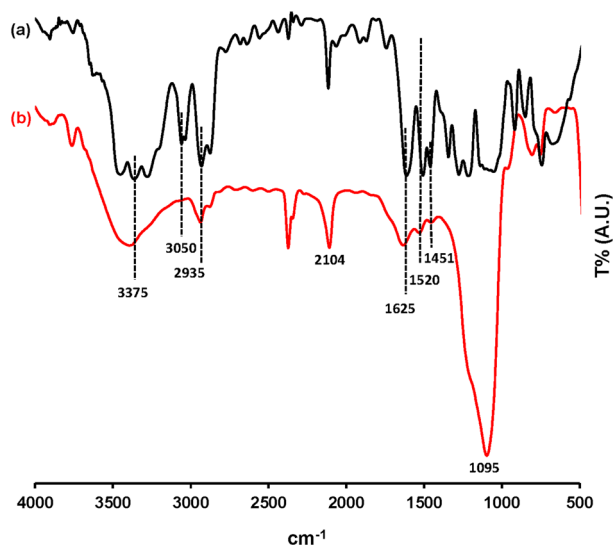
Scheme 3 Synthesis of MNP@SiO$_2$-SBA-DPPE-Pd(II)

Fig. 3 FT-IR spectra (KBr) of: (a) DPPE; and (b) MNP@SiO$_2$@ SBA-DPPE

Table 1 FT-IR characteristic absorptions of DPPE and MNP@SiO$_2$-SBA-DPPE-Pd(II)

Entry	Functional group	Absorption (cm^{-1})	References
1	Fe–O (stretching)	560	[25]
2	Si–O (stretching)	1095	[8]
3	C=C (stretching, aromatic)	1451, 1520	[40, 41]
4	N–H (bending)	1625	[42]
5	C–H (stretching, aliphatic)	2935	[43]
6	C–H (stretching, aromatic)	3050	[44]
7	NH$_2$ (stretching)	3375	[42]

easily separated from the reaction medium, recycled, and re-used many times without significant loss of activity.
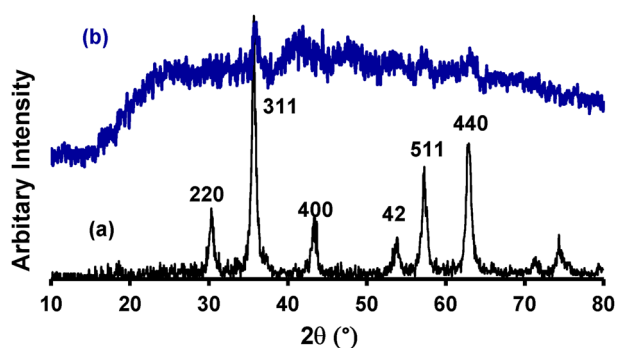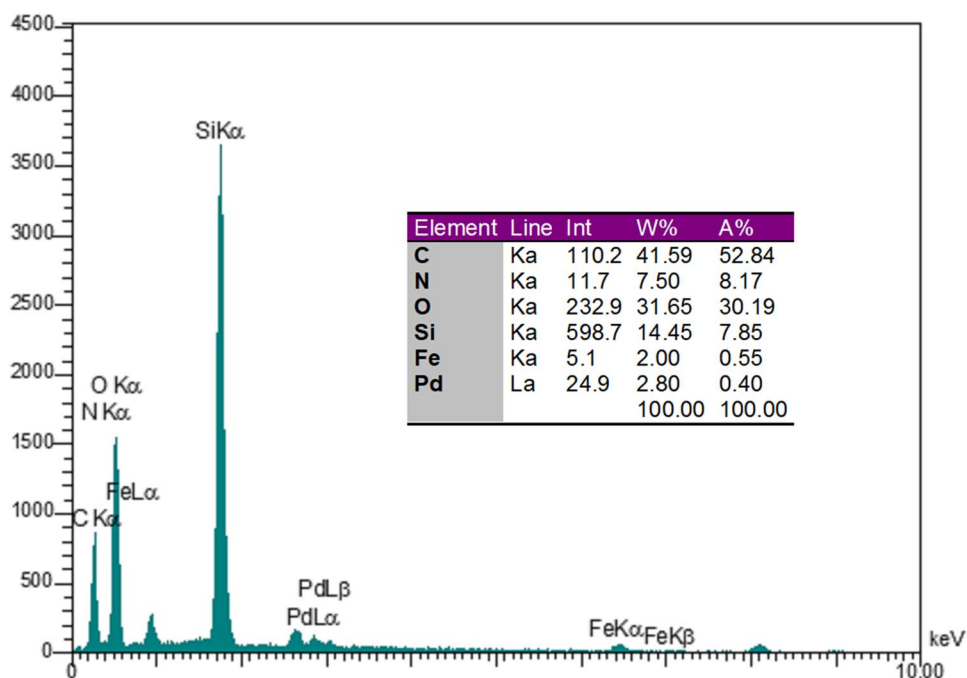
2 Experimental

2.1 Materials

MNP@SiO$_2$-SBA magnetic composite [28] and 3-azidopropyltriethoxysilane [29] were prepared according to reported methods in the literature. 1,3-Di-(*o*-nitrophenoxy)-2-propanol (1) was synthesized via the method described by Zhang et al. [30] via the reaction of *o*-nitrophenol and 1,3-dichloro-2-propanol in boiling DMF and in the presence of K$_2$CO$_3$. Laboratory grade solvents used in this work were dried according to reported procedures in the literature [31]. The remaining chemicals were obtained from Merck and used as received.

2.2 Synthesis of 1,3-Di-(*o*-nitrophenoxy)-2-Propyl Propargyl Ether (3)

To a stirred solution of 1,3-di-(*o*-nitrophenoxy)-2-propanol 1 (0.830 g, 2.5 mmol) in dry DMF (5 ml) at 0 °C was added NaH (0.132 g, 3 mmol; 60% dispersion in mineral oil) in small portions under argon. The mixture was stirred in an ice bath for 1 h and then propargyl bromide (0.31 ml, 6 mmol) was added dropwise. The reaction mixture was warmed to room temperature, stirred for additional 10 h, and quenched by MeOH (7 ml). The white precipitate was filtered in vacuum, washed cold EtOH and dried to give 0.630 g product [32]. (Yield: 66%, mp: 100–103 °C). FT-IR (KBr, cm^{-1}): 3269 (m), 3061 (w), 2932 (w), 2869 (w), 1607 (m), 1521 (s), 1350 (s), 1280 (m), 1250 (m), 743 (m).

2.3 Synthesis of 1,3-Di-(*o*-aminophenoxy)-2-Propyl Propargyl Ether (DPPE)

To a rapidly stirred suspension of powdered zinc (1.740 g, 26.6 mmol) in 4.25 ml of 37% aqueous ammonia was added

Fig. 4 EDX analysis of MNP@SiO$_2$-SBA-DPPE Pd(II)

Element	Line	Int	W%	A%
C	Ka	110.2	41.59	52.84
N	Ka	11.7	7.50	8.17
O	Ka	232.9	31.65	30.19
Si	Ka	598.7	14.45	7.85
Fe	Ka	5.1	2.00	0.55
Pd	La	24.9	2.80	0.40
			100.00	100.00

Fig. 5 Wide angle powder XRD patterns of of: (a) MNP@SiO$_2$-SBA; and (b) MNP@SiO$_2$-SBA-DPPE Pd(II)

a solution of 3 (1.000 g, 2.65 mmol) in 4.25 ml of THF. The mixture was refluxed for 6 h and then filtered. The filtrate was extracted with three 15 ml portions of ethyl acetate/water (50:50) mixture, and the combined extracts evaporated to dryness. The obtained residual orange oil chromatographed on 20 cm×20 cm silica gel covered glass plates using 75:25 petroleum ether/acetone eluent to afford to give 0.510 g of orange oily product [33]. (Yield: 38%). FT-IR (KBr, cm^{-1}): 3294 (s), 3048 (w), 2935 (w), 2869 (w), 1648 (s), 1526 (m), 1448 (w), 1310 (w), 1032 (m), 735 (m). ^{1}H-NMR (250 MHz, CDCl$_3$ δ): 6.85–7.00 (m, 2H); 6.70–6.80 (m, 2H); 4.47–4.50 (m, 2H); 4.40–4.46 (m, 1H); 4.23–4.32 (m, 4H); 3.90 (br, s, 4H); 2.54–2.56 (m, 1H). ^{13}CNMR

(62.5 MHz, CDCl$_3$,δ): 141.1 (<u>C</u>–O, Ar.), 136.6 (<u>C</u>–N, Ar.), 122.0, 118.5, 115.4, 112.2, 79.8 (<u>C</u>H–O), 75.5 (≡C–<u>C</u> H$_2$), 75.1 (≡<u>C</u>–H), 68.3 (O–<u>C</u>H$_2$–CH), 57.9 (≡C–<u>C</u> H$_2$). Mass: (m/z)$^+$: 312.15 (M$^+$, 84%).

2.4 Synthesis of Azide Functionalized Magnetic Nanocomposite MNP@SiO$_2$-SBA-N$_3$

A suspension of MNP@SiO$_2$-SBA (1.000 g) in 50 ml of toluene was irradiated in an ultrasonic bath for 10 min. To this suspension, 3-azidopropyltriethoxysilane (2.0 ml, 9.7 mmol) was added, and the mixture was stirred for 16 h at 80 °C under argon. The reaction mixture was then cooled, filtered and washed with toluene several times and then dried at 45 °C in a vacuum oven [29]. FT-IR (KBr, cm^{-1}): 2935 (w), 2869 (w), 2104 (m), 1628 (m), 1526 (w), 1448 (w), 1088 (s), 735 (m).

2.5 Synthesis of MNP@SiO$_2$-SBA-DPPE via Click Reaction

In a round-bottomed flask MNP@SiO$_2$-SBA-N$_3$ (1.000 g) was dispersed in 20 ml of *t*-BuOH/water (1:1) containing CuSO$_4$ (0.330 g, 1.32 mmol), sodium ascorbate (1.070 g, 5.4 mmol) and DPPE (1.200 g, 4.8 mmol). The mixture was irradiated in an ultrasonic bath for 15 min and stirred at 80 °C for 24 h under argon. The magnetic particles were then magnetically decanted, washed with EtOH and then dried in a vacuum oven at 80 °C [29]. FT-IR (KBr, cm^{-1}): 3397 (br, s), 3067 (w), 2935 (w), 2869 (w), 2104 (m), 1628 (m), 1526 (w), 1448 (w), 1088 (s), 735 (m).
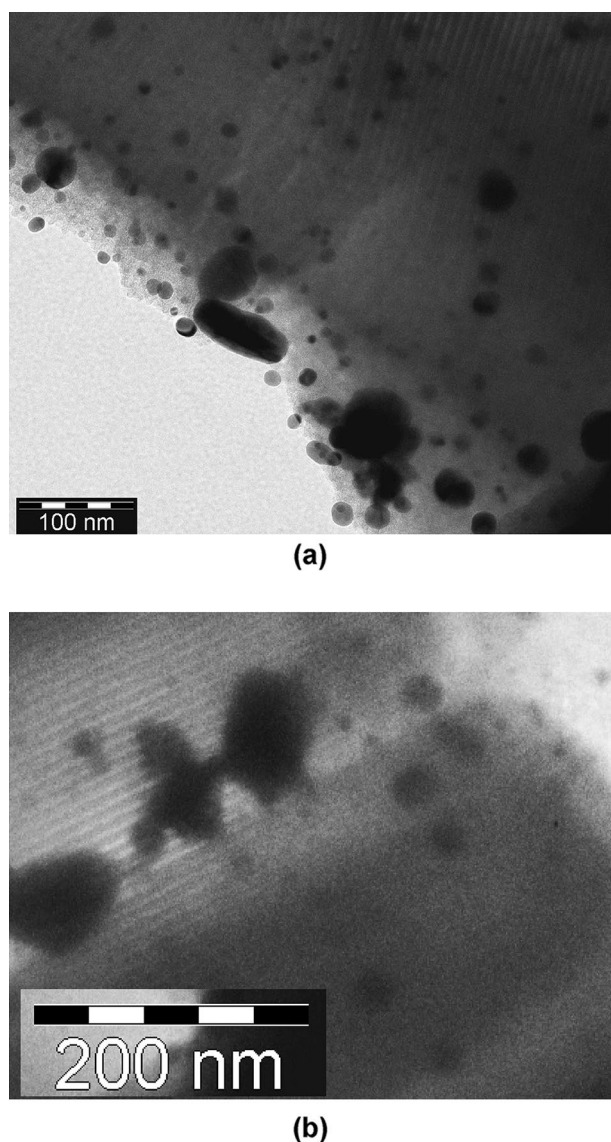
(a)

(b)

Fig. 6 TEM images of magnetic SBA

2.6 Synthesis of MNP@SiO₂-SBA-DPPE-Pd(II)

DPPE functionalized magnetic mesoporous silica particles (1.000 g) were dispersed in a $PdCl_2$ (0.03 g, 0.17 mmol) solution in EtOH (8 ml) in an ultrasonic bath for 15 min, and then stirred at room temperature for 12 h. The catalyst was decanted magnetically, washed several times with EtOH and then dried in vacuum at 45 °C [34].

2.7 General Procedure for the Heck Reaction

Typically, the supported catalyst (1.10 mol%) was dispersed in 1 ml N-methyl-2-pyrrolidone (NMP) through 8 min ultra-sonication. Olefin (1.00 mmol), aryl halide (1.00 mmol), and K_2CO_3 (1.5 mmol) were then added and the reaction

mixture was stirred at 120 °C. The catalyst was magnetically decanted as the reaction was completed (followed by TLC) and the mixture was analyzed by GC. The samples for NMR analysis were chromatographed on glass plates covered by silica gel.

3 Results and Discussion

3.1 Preparation and Characterization of the Catalyst

The new ligand (DPPE) has been prepared in two steps as shown in Scheme 2. In the first step, 1,3-di-(*o*-aminophenoxy)-2-propanol (1) was etherified with propargyl bromide 2 [32]. Selective reduction of nitro groups in the presence of ethynyl group by conventionl methods such as Pd/C/hydrazine; Pd/C/NaBH₄; Fe/HCl; Sn/HCl, and Zn/HCl were unsuccessful. This was done by the specific method described by Kovar and Arnold for preparation of the ethy-nyl substuted *o*-diamines [33].

Common spectroscopy methods were applied to confirm the structure of DPPE. In the mass spectrum (Fig. 1), molecular ion peak appears at $m/e = 312.15$ (84%).

Figure 2a and b present the ¹H NMR and ¹³C NMR spectra of DPPE, respectively. As Fig. 1a shows, the acetylenic proton is observed as a multiplet at 2.54–2.56 ppm. The protons related to amino groups and methylenes adjacent to oxygens of the aromatic rings appear as a broad singlet centered at 3.90 ppm, and a multiplet at 4.23–4.32 ppm, respectively. The protons of chiral carbon and methylene group adjacent to C≡C bond are seen as two multiplets at 4.40–4.47 ppm and 4.47–4.50 ppm, respectively. The aromatic rings protons appear at 6.70–6.80 ppm. In Fig. 2b, the observed 11 signals are compatible with the structure of DPPE. The prepared ligand can be supported on the surface of metal oxides via a simple click reaction.

Magnetite nanoparticles were prepared via co-precipitation method and then covered by a silica layer and then embedded into mesoporous silica (SBA-15) [28]. The combination of SBA-15 porous structure with the magnetic property of MNPs provides high density of catalytic sites for enhanced activity along with the advantage of simple magnetic decantation of the catalyst at the end of reaction. The as-prepared MNP@SiO₂-SBA particles were then silylated with 3-azidopropyltrimethoxysilane via post-synthesis grafting technique described by Malvi et al. [29]. The azide functionalized magnetic mesoporous silica was further functionalized with DPPE via the click methodology, and then treated with PdCl₂ solution in EtOH to afford supported Pd(II)-complex, Scheme 3.

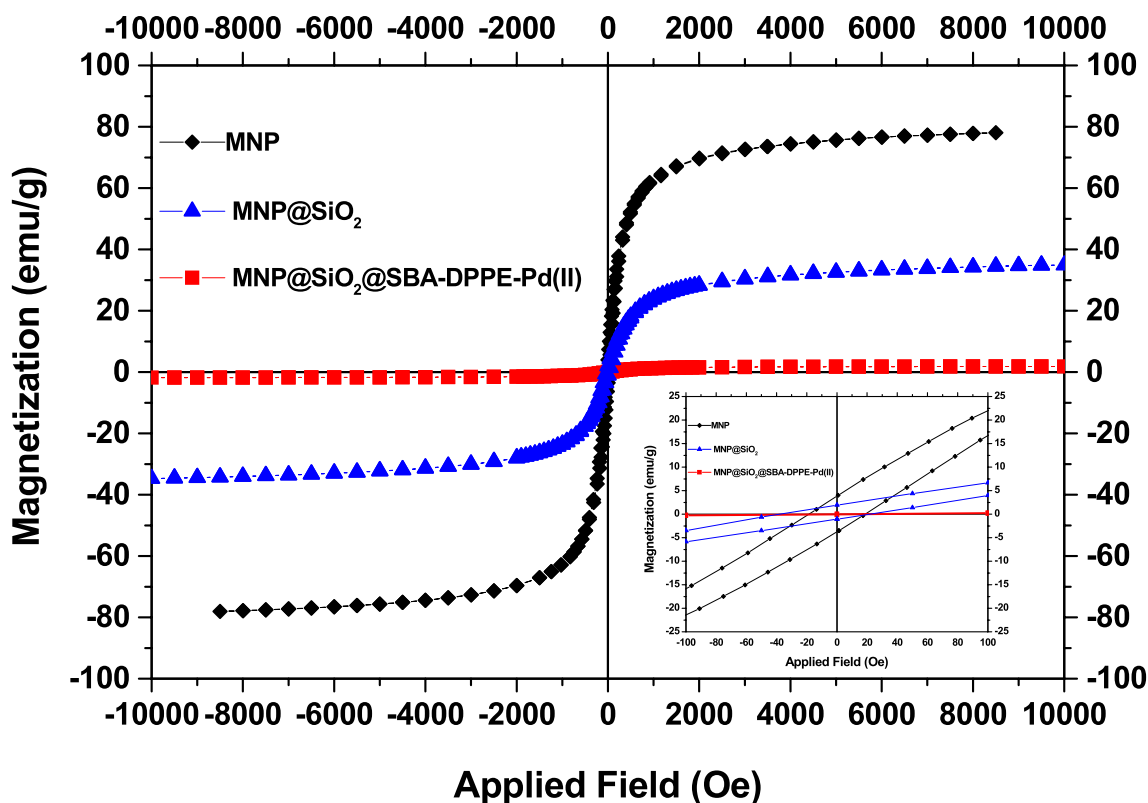The FT-IR spectra of DPPE and MNP@SiO₂-SBA-DPPE are shown in Fig. 3a and b. Figure 3b shows the

Fig. 7 Magnetization curves for the MNP, MNP@SiO$_2$ and MNP@SiO$_2$-SBA-DPPE-Pd(II)

Table 2 Magnetic properties of the prepared materials

Sample	M_s^a (emu g^{-1})	M_r^b (emu g^{-1})	H_c^c (Oe)	M_r/M_s^d
MNPs	78.14	4.03	18.6	0.05
MNP@SiO$_2$	34.52	1.91	22.2	0.06
MNP@SiO$_2$@ SBA@DPPE- Pd(II)	1.56	0.08	29.6	0.05

^{a}Saturation magnetization

^{b}Remanent magnetization

^{c}Coercive force

^{d}Remanence ratio

characteristic peak of magnetite at 560 cm^{-1}. The strong absorption band observed at 1095 cm^{-1} (ν_{as} Si–O–Si) reveals the formation of MNP@SiO$_2$ nano-composite [8]. Figure 3b clearly shows the characteristic peaks related to the ligand. The adsorption bands observed at 1451 cm^{-1}, and 1520 cm^{-1} are related to C=C stretching vibrations of aromatic ring. The N–H bending vibration appeared at 1625 cm^{-1}. The stretching vibrations related to aliphatic C–H, aromatic C–H, and NH$_2$ groups appear at 2935 cm^{-1}, 3050 cm^{-1}, and 3375 cm^{-1}, respectively. The FT-IR data are summarized in Table 1.

Surface qualitative elemental analysis at random points by EDX confirmed the presence of palladium atoms, Fig. 4. In addition, the EDX spectrum shows the signals of carbon, nitrogen, oxygen, silicon, and iron, and the presence of these elements in the supported catalyst. Atomic absorption spectroscopy revealed that the palladium loading is 0.10 mmol g^{-1} (1.10 wt%).

Figure 5a and b shows the XRD patterns of MNP and MNP@SiO$_2$-SBA-DPPE-Pd(II). Both samples exhibit well-resolved diffraction peaks that can be indexed as (220), (311), (400), (422), (511) and (440) planes associated with cubic magnetite nanoparticles (JCPDS-ICDD Copyright 1938, file No. 01–1111) with the Fd − 3 m space group [35]. However, due to reposing of MNPs between the channels of mesoporous silica, intensities of these characteristic diffraction peaks were attenuated in the pattern of supported catalyst, Fig. 5b.

The image obtained by TEM also confirmed ordered structure of magnetic SBA (Fig. 6). Highly ordered arrays of 1D mesoporous channels in which MNPs with 20 to 50 nm diameter are located between the channels of MNP@SiO$_2$@ SBA are seen in this image.

Figure 7 shows the hysteresis loops of MNP, MNP@SiO$_2$ and MNP@SiO$_2$-SBA-DPPE-Pd(II) at room temperature and the results are tabulated in Table 2. Superparamagnetic

Table 3 Optimization of conditions for Heck reaction
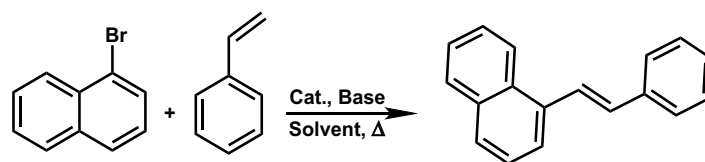
Entry	Solvent	Pd (mol%)	Base	Temperature (°C)	Conversion (%)[a]	TON[b]/TOF (h^{-1})[c]
1	EtOAc	0.1	K_2CO_3	60	Trace	–
2	Ethanol	0.1	K_2CO_3	60	Trace	–
3	CHCl$_3$	0.1	K_2CO_3	60	Trace	
4	Acetone	0.1	K_2CO_3	60	Trace	–
5	DMF	0.1	K_2CO_3	120	60	
6	DMAc	0.1	K_2CO_3	120	53	529/176
7	DMSO	0.1	K_2CO_3	120	Trace	–
8	H$_2$O	0.1	K_2CO_3	60	22	
9	**NMP**	**0.1**	**K_2CO_3**	**120**	**90**	**901/300**
10	NMP	0.1	Et$_3$N	120	52	520/173
11	NMP	0.1	Cs$_2$CO$_3$	120	22	220/73
12	NMP	0.1	Pyridine	120	Trace	–
13	NMP	0.1	NaOAc	120	61	
14	NMP	0.1	K_2CO_3[d]	120	64	637/212
15	NMP	0.1	K_2CO_3[e]	120	71	709/236
16	NMP	0.07	K_2CO_3	120	36	363/121
17	NMP	0.15	K_2CO_3	120	55	548/182
18	NMP	0.2	K_2CO_3	120	47	472/157
19	NMP	0.1	K_2CO_3	80	Trace	–
20	NMP	0.1	K_2CO_3	100	1	
21	NMP	0.1	K_2CO_3	140	88	880/293
22	NMP	–	K_2CO_3	120	–	–

Optimal reaction conditions are highlighted in bold

Reaction conditions: 1-Bromonaphthalene (1.0 mmol), styrene (1.0 mmol), solvent (1 ml), base (1.5 mmol) and reaction time 3.0 h

[a]Determined by GC analysis

[b]Turn over number: TON = The number of moles of desired product/the number of moles of metal active sites

[c]Turn over frequency: TOF = The number of moles of reactant converted/(The number of moles of metal active sites × Time in hours)

[d]1.0 mmol

[e]2.0 mmol

behavior of the samples is shown by small remanence, hysteresis, coercivity values, and narrow width of the loop as seen in the inset of Fig. 7 [36, 37]. The saturation magnetizations of MNP, MNP@SiO$_2$ and MNP@SiO$_2$-SBA-DPPE-Pd(II) are 78.14, 34.52, and 1.56 emu g^{-1}, respectively. Dropping of the maximal saturation magnetization of supported catalyst may be due to the entangling of MNPs between SBA channels.

3.2 Heck Coupling Reaction

Styrene and 1-bromonaphthalene were chosen as the model compounds for optimizing the Heck coupling reaction conditions. Reaction parameters such as the solvent, base, amount of base, amount of catalyst, and reaction temperature were studied. The results are shown in Table 3 and Fig. 8a–c. According to solvent screening (Entries 1 to 9), the NMP solvent is the best choice due to the highest yield (Entry 9, 90% yield). The effect of the base and its quantity were also evaluated (Entries 9 to 13). The highest conversion is achieved with the K$_2$CO$_3$ base (Entry 9, 90% yield). Higher
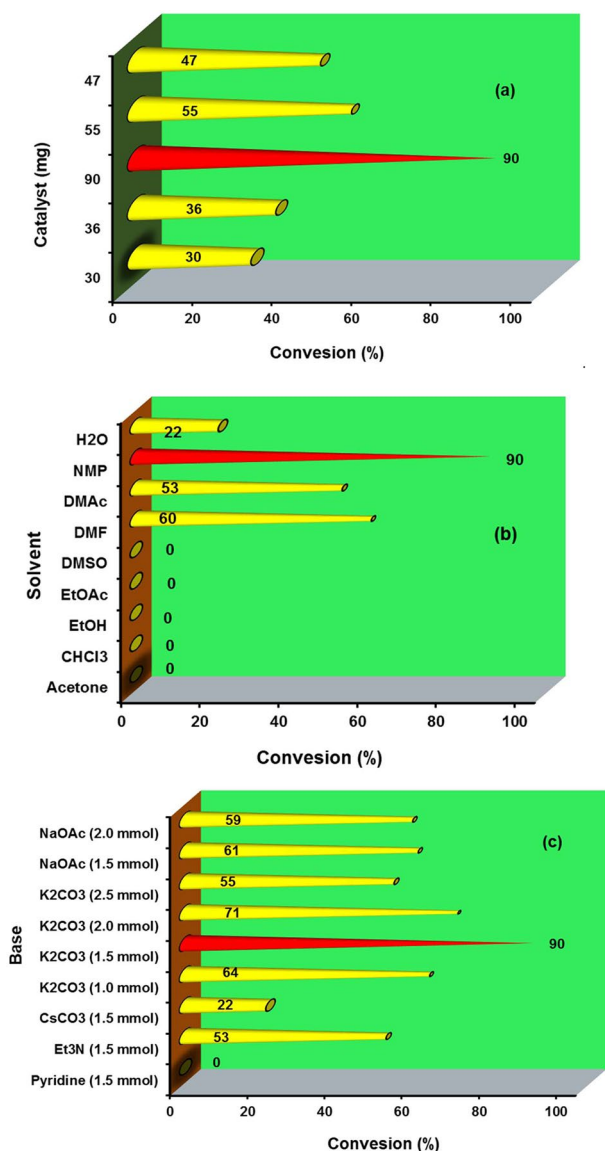
Fig. 8 Optimization of the Heck reaction conditions: **a** solvent; **b** catalyst loading; and **c** Base. Reaction conditions: 1-Bromonaphthalene (1.0 mmol), styrene (1.0 mmol), solvent (1 ml)

or lower quantities of the base than that of 1.5 molar ratio diminish the reaction conversion (Entries 14 and 15). The optimization of catalyst dosage shows that using the catalyst containing 0.1 mol% Pd(II) is the optimal value (Entry 9, 90% yield). It should be noted that the reaction does not proceed properly at the temperatures lower or higher than 120 °C (Entries 19 to 21) and in the absence of the catalyst (Entry 22).

Various aryl halides were subjected to the optimized reaction conditions with different olefins, Table 4. As shown, aryl iodides and aryl bromides showed excellent conversions and TOFs (Entries 1 to 13), excluding 2-bromopyridine (Entry 13, conversion 34%). Aryl chlorides showed

moderate reactivity under the applied reaction conditions excluding chlorobenzene (Entries 14 to 16).

A possible mechanism for the Heck cross-coupling reaction catalyzed by a supported Pd(II) complex can be proposed as Scheme 4. The mechanism is suggested based on the mechanism described by Shaw et al. [38, 39], in which a Pd(II)/Pd(IV) cycle is involved. In the proposed mechanism, olefin coordinates of to the supported Pd(II), and then an alkyl σ-complex is formed by attacking the nucleophile (KCO_3^-) on the coordinated complex. The aryl halide oxidizes the Pd(II) center, the attached nucleophile is released and the alkene coordinates to the Pd(IV) complex, again. The catalyst is regenerated via β-hydride elimination and base-induced removal of hydrogen halide that gives the desired product.

3.3 Characterization of the Recycled Catalyst

In order to indicate the stability of MNP@SiO_2-SBA-DPPE-Pd(II), after using in the coupling reaction of bromonaphthalene and styrene, the catalyst was collected and characterized by FT-IR, Fig. 9a and b. As seen, the spectra of the recovered catalyst does not show any significant changes in comparison with the fresh catalyst.

3.4 Comparison of the Catalyst

The comparison of the prepared magnetic catalyst with a few literature reported catalysts in the coupling reaction of iodobenzene with styrene reveals that our prepared magnetic catalyst has enhanced reactivity, Table 5. In addition, the mesoporous structure of the prepared catlyst provides a very high srface area in compared with the most catalysts listed in Table 5. The prepared catlyst has also enjoys the benefit of magnetic separation and easy recovering process as the major advantage. High thermal stability is an other advantage of the our prepared catlyst over the catalysts listed catalyst in Table 5.
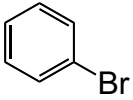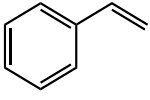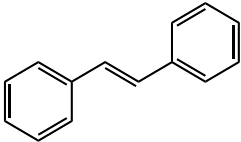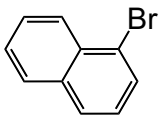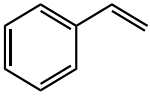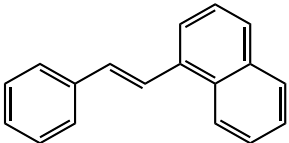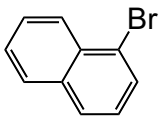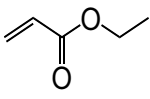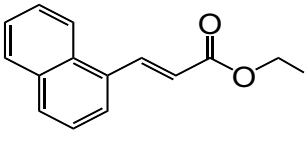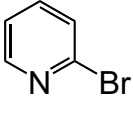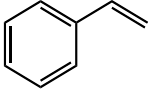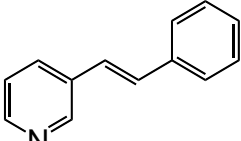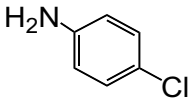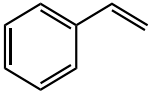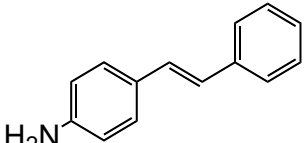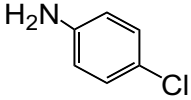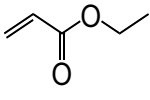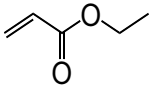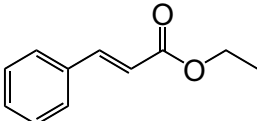
3.5 Recyclability of the Catalyst

Supported catalysts are usually prepared via complicated and expensive routes. Therefore, it is necessary to pay sufficient attention to retrieving of a used catalyst. The stability and re-usability of the magnetic catalyst were tested in the Heck coupling reactions of 1-bromonaphthalene and ethyl acrylate, Fig. 10. After each r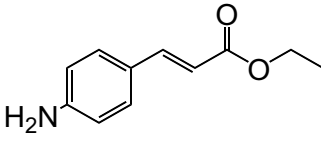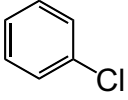eaction, the catalyst was collected magnetically, washed with ethyl acetate, and then dried. As shown, the conversion reaches to 97.3% in the first run and then slightly dropped to 90.1% during five consecutive runs of the Heck reaction. Therefore, it can be concluded that the prepared supported catalyst is active and recyclable.

Table 4 Heck reaction of aryl halide with olefin catalyzed by the supported Pd(II) complex
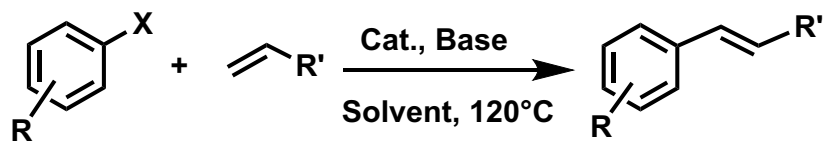
Entry	Aryl halide	Olefin	Product	m.p. (°C)		Time (h)	TON/TOF (h^{-1})	Conversion (%)
				Found	Reported [Ref.]			
1				Oil	Oil [45]	2	962/320	96
2				118–120	118–121 [46]	2	971/324	97
3				74–76	76–78 [47]	3	965/321	97
4				Oil	Oil [48]	3	929/309	93
5				Oil	Oil	2	865/288	87
6				145–147	148–150 [49]	4	764/254	76
7				151–152	151–153 [18]	18	601/200	60
8				70–72	72–74 [17]	4	575/191	58
9				Oil	Oil [45]	2	536/178	54

Table 4 (continued)

Entry	Aryl halide	Olefin	Product	m.p. (°C)		Time (h)	TON/TOF (h⁻¹)	Conversion (%)
				Found	Reported [Ref.]			
10				118–120	118–121 [46]	2	501/167	50
11				71–73	70–71 [49]	3	901/300	90
12				78–79	80–81 [50]	4	972/324	97
13				77–78	78–79 [26]	18	335/111	34
14				151–152	151–153 [18]	18	427/142	43
15				70–72	72–74 [17]	18	408/136	40.8
16				37–39	36–38 [45]	18	–	Trace

Reaction conditions: Aryl halide (1.0 mmol), olefin (1.0 mmol), solvent (1.0 ml), Pd(II) (0.1 mol%), and base (1.5 mmol)

3.6 Leaching Study

In order to confirm the stability and heterogeneous nature of MNP@SiO$_2$-SBA-DPPE-Pd(II), after using in the coupling reaction of bromonaphthalene and styrene, the catalyst was collected. The palladium concentration was measured in the remaining aliquat by atomic absorption which was found to be 0.0000116 mmol ml⁻¹. The very low Pd concentration proves that no considerable metal leaching occurred in the reaction medium. Therefore, the heterogeneous palladium is responsible for completion of the reaction.
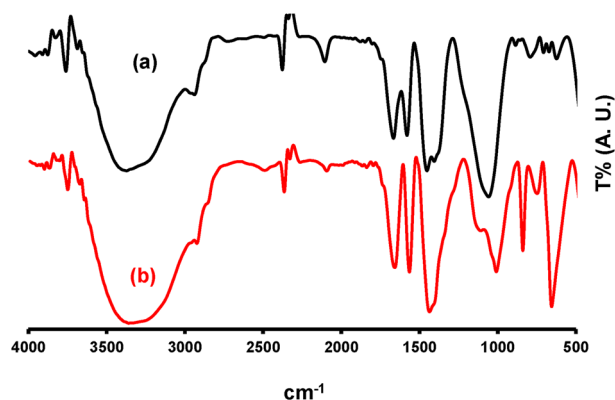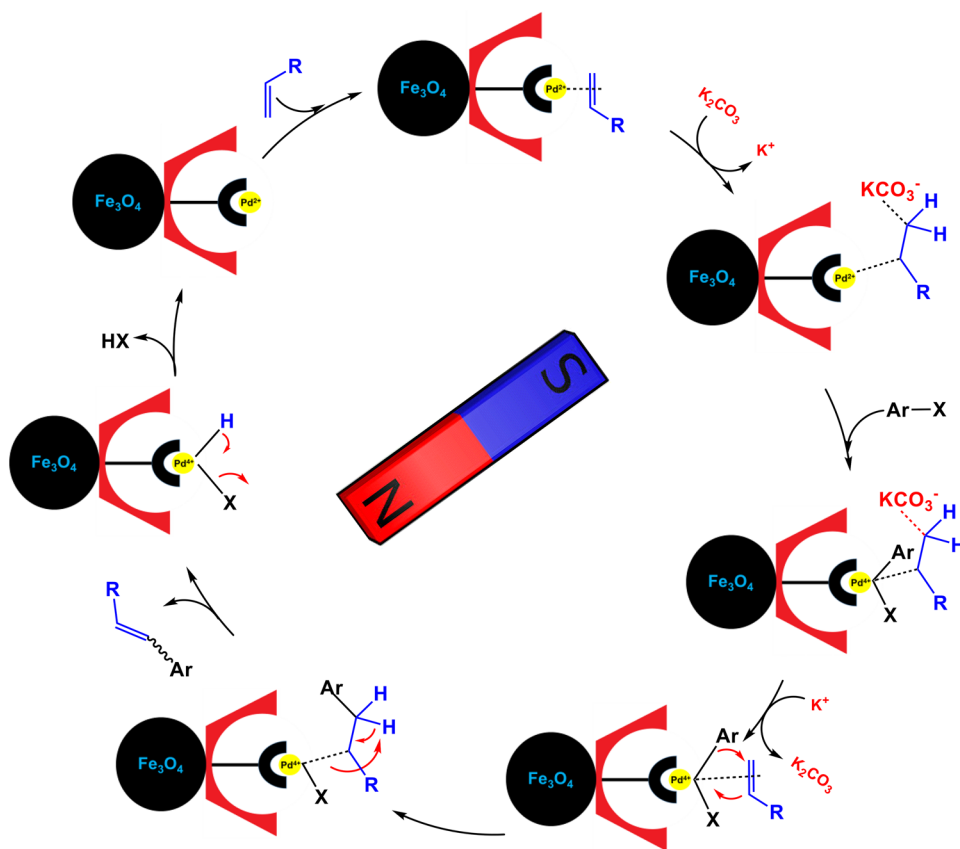
Fig. 9 FT-IR spectra of: (a) recovered MNP@SiO$_2$-SBA-DPPE-Pd(II) and; (b) Fresh MNP@SiO$_2$-SBA-DPPE-Pd(II)

4 Conclusion

In summary, the synthesis, characterization, and application of an efficient and retrievable magnetic catalyst are reported. The catalyst was obtained by supporting a Pd(II) complex on magnetic mesoporous silica. For this purpose, DPPE was synthesized, characterized, and then supported on magnetic SBA via the click reaction. The supported ligand was treated with a Pd(II) solution to afford a supported Pd(II) catalyst. The obtained magnetic catalyst was fully characterized by the FT-IR, TGA, SEM, TEM, XRD, EDX, BET, and VSM analyses. It was shown that, the prepared catalyst could efficiently catalyze the Heck cross-coupling reaction of aryl halides and olefins. Excellent conversions were obtained and the recovering ability of the catalyst was shown by magnetic separation and re-using of the recovered catalyst. The recovered catalyst was reused several times with significant deactivation.

Table 5 Comparison of the prepared catalyst with other catalysts for Heck cross-coupling reactions from iodobenzene with styrene

Entry	Catalyst	Conditions	Time (h)	Yield (%)	TOF (h^{-1})	References
1	Agarose-Pd(0)	Solvent free, Et$_3$N, 120 °C	2.0	90	87	[51]
2	PdNP-SβCD	H$_2$O, K$_2$CO$_3$, 100 °C	2.0	99	91	[52]
3	Palladacycle	DMA, Et$_3$N, 140 °C	18.0	100	28	[53]
4	Pd/C particles	H$_2$O, Et$_3$N, 100 °C	24	23	0.2	[54]
5	Pd–MPTA-1	H$_2$O, Cs$_2$CO$_3$, 100 °C	6.0	92	217	[55]
6	Pd(OAc)$_2$ (ligand Free)	PEG-400, CH$_3$COONa, 80 °C	1.5	93	62	[56]
7	1′-Carbopalladated complexes	Et$_3$N, DMA, 80 °C	3.0	80	53	[57]
8	The supported NHC Pd(II) complex	NMP, K$_2$CO$_3$, 120 °C	2	96	192	[25]
9[a]	Pd-imi@MCM-41/Fe$_3$O$_4$	PEG-400, Na$_2$CO$_3$, 120 °C	0.8	95	78	[19]
10	MNP@SiO$_2$-SBA-DPPE-Pd(II)	NMP, K$_2$CO$_3$, 120 °C	1.0	97	324	This work

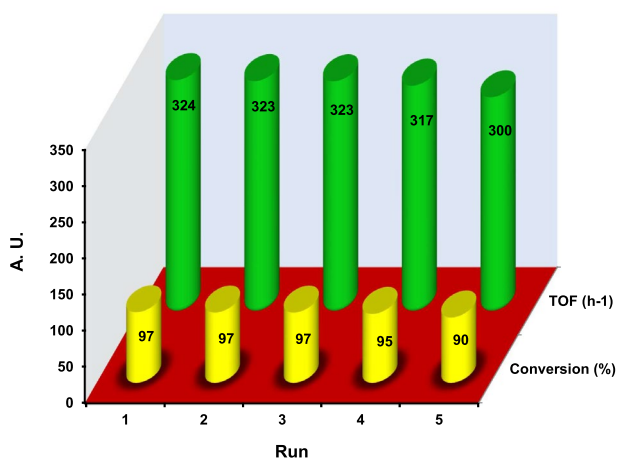[a]The investigation was studied for the Heck cross-coupling reaction of iodobenzene and methylacrylate

Fig. 10 Recycling of MNP@SiO$_2$-SBA-DPPE-Pd(II) for the Heck cross-coupling reaction of 1-bromonaphthalene and ethylacrylate

References

1. Chen Y, Wang M, Zhang L, Liu Y, Han J (2017) RSC Adv 7:47104
2. Tsutomu M, Kunio M, Atsumu O (1971) Bull Chem Soc Jpn 44:581
3. Heck RF, Nolley JP (1972) J Org Chem 37:2320
4. Nasrollahzadeh M, Issaabadi Z, Tohidi MM, Mohammad Sajadi S (2018) Chem Rec 18:165
5. Beletskaya IP, Cheprakov AV (2000) Chem Rev 100:3009
6. C.P. Mehnert, J. Y. Ying, Chem Commun, 2215 (1997)
7. Polshettiwar V, Molnár Á (2007) Tetrahedron 63:6949
8. Kang T, Li F, Baik S, Shao W, Ling D, Hyeon T (2017) Biomaterials 136:98
9. Moon SH, Noh S-H, Lee J-H, Shin T-H, Lim Y, Cheon J (2017) Nano Lett 17:800
10. Tayeb Oskoie P, Mansoori Y (2018) J Part Sci Technol 4:1
11. Rahimi L, Mansoori Y, Nuri A, Esquivel D (2020) ChemistrySelect 5:11690
12. Arnaudov M (1999) Spectrosc Lett 32:165
13. Baig RN, Varma RS (2013) Chem Commun 49:752
14. Nuri A, Mansoori Y, Bezaatpour A, Shchukarev A, Mikkola J-P (2019) ChemistrySelect 4:1820
15. Rutnakornpituk M, Puangsin N, Theamdee P, Rutnakornpituk B, Wichai U (2011) Polymer 52:987
16. Donescu D, Raditoiu V, Spataru CI, Somoghi R, Ghiurea M, Radovici C, Fierascu RC, Schinteie G, Leca A, Kuncser V (2012) Eur Polym J 48:1709
17. Yasuhara A, Kasano A, Sakamoto T (1999) J Org Chem 64:2301
18. Yang J-S, Wang C-M, Hwang C-Y, Liau K-L, Chiou S-Y (2003) Photochem Photobiol Sci 2:1225
19. Ghorbani-Choghamarani A, Tahmasbi B, Hudson RHE, Heidari A (2019) Microporous Mesoporous Mater 284:366
20. Tahmasbi B, Ghorbani-Choghamarani A (2019) New J Chem 43:14485
21. Martínez-Edo G, Balmori A, Pontón I, Martí del Rio A, Sánchez-García D (2018) Catalysts 8:617
22. Fu Y, Sun Y, Chen Z, Ying S, Wang J, Hu J (2019) Sci Total Environ 691:664
23. Jiang W, Jia H, Fan X, Dong L, Guo T, Zhu L, Zhu W, Li H (2019) Appl Surf Sci 484:1027
24. Sorokina SA, Kuchkina NV, Lawson BP, Krasnova IY, Nemygina NA, Nikoshvili LZ, Talanova VN, Stein BD, Pink M, Morgan DG, Sulman EM, Bronstein LM, Shifrina ZB (2019) Appl Surf Sci 488:865
25. Nuri A, Mansoori Y, Bezaatpour A (2019) Appl Organomet Chem 33:e4904
26. Kanagaraj K, Pitchumani K (2013) Chem Eur J 19:14425
27. Nuri A, Vucetic N, Smått J-H, Mansoori Y, Mikkola J-P, Murzin DY (2019) Catal. Lett. 149(7):1941–1951
28. Wang S, Wang K, Dai C, Shi H, Li J (2015) Chem Eng J 262:897
29. Malvi B, Sarkar BR, Pati D, Mathew R, Ajithkumar TG, Sen Gupta S (2009) J Mater Chem 19:1409
30. Zhang W, Liu S, Ma C, Jiang D (1998) Polyhedron 17:3835
31. Armarego WLF, Chai CLL (2003) Purification of laboratory chemicals, 5th edn. Butterworth-Heinemann, Burlington
32. Lv G, Mai W, Jin R, Gao L (2008) Synlett 2008:1418
33. R.F. Kovar, F.E. Arnold, US Patent 3,975,444 (1976)
34. Peng X, Zhao Y, Yang T, Yang Y, Jiang Y, Ma Z, Li X, Hou J, Xi B, Liu H (2018) Microporous Mesoporous Mater 258:26
35. Hanawalt JD, Rinn HW, Frevel LK (1938) Ind Eng Chem Anal Ed 10:457

36. Choubey J, Bajpai AK (2010) J Mater Sci Mater Med 21:1573
37. Basavaraja C, Jo EA, Huh DS (2010) Mater Lett 64:762
38. B.L. Shaw, Chem Commun, 1361 (1998)
39. Shaw B (1998) New J Chem 22:77
40. Nieva Lobos ML, Sieben JM, Comignani V, Duarte M, Volpe MA, Moyano EL (2016) Int J Hydrogen Energy 41:10695
41. Moradi P, Hajjami M, Tahmasbi B (2020) Polyhedron 175:114169
42. Danon A, Stair PC, Weitz E (2011) J Phys Chem C 115:11540
43. Mansoori Y, Khodayari A, Banaei A, Mirzaeinejad M, Azizian-Kalandaragh Y, Pooresmaeil M (2016) RSC Adv 6:48676
44. Rahmaninia A, Mansoori Y, Nasiri F, Bezaatpour A, Babaei B (2019) J Part Sci Technol 5:47
45. Sun P, Zhu Y, Yang H, Yan H, Lu L, Zhang X, Mao J (2012) Org Biomol Chem 10:4512
46. Górski B, Talko A, Basak T, Barbasiewicz M (2017) Org Lett 19:1756
47. Inomata S, Hiroki H, Terashima T, Ogata K, Fukuzawa S (2011) Tetrahedron 67:7263
48. Huang S-H, Chen J-R, Tsai F-Y (2010) Molecules 15:315
49. Yu L, Huang Y, Wei Z, Ding Y, Su C, Xu Q (2015) J Org Chem 80:8677
50. Prevost MS, Delarue-Cochin S, Marteaux J, Colas C, Van Renterghem C, Blondel A, Malliavin T, Corringer P-J, Joseph D (2013) J Med Chem 56:4619
51. Firouzabadi H, Iranpoor N, Kazemi F, Gholinejad M (2012) J Mol Catal A Chem 357:154
52. Khalafi-Nezhad A, Panahi F (2014) ACS Sustain Chem Eng 2:1177
53. Gruber AS, Zim D, Ebeling G, Monteiro AL, Dupont J (2000) Org Lett 2:1287
54. Cassez A, Kania N, Hapiot F, Fourmentin S, Monflier E, Ponchel A (2008) Catal Commun 9:1346
55. Mondal J, Modak A, Bhaumik A (2011) J Mol Catal A Chem 350:40
56. Han W, Liu N, Liu C, Jin ZL (2010) Chin Chem Lett 21:1411
57. Rosol M, Moyano A (2005) J Organomet Chem 690:2291